ELSEVIER

Molecular & Biochemical Parasitology 118 (2001) 61–73

MOLECULAR & BIOCHEMICAL PARASITOLOGY

www.parasitology-online.com.

Active site mapping, biochemical properties and subcellular localization of rhodesain, the major cysteine protease of *Trypanosoma brucei rhodesiense*☆

Conor R. Caffrey [a], Elizabeth Hansell [a], Kimberley D. Lucas [a], Linda S. Brinen [a], Alejandro Alvarez Hernandez [b], Jiamning Cheng [b], Stephen L. Gwaltney II [b], William R. Roush [b], York-Dieter Stierhof [c], Matthew Bogyo [d], Dietmar Steverding [e], James H. McKerrow [a,*]

[a] *Tropical Disease Research Unit, Department of Pathology, University of California San Francisco, VAMC, 4150 Clement Street-113B, San Francisco, CA 94121, USA*

[b] *Department of Chemistry, University of Michigan, Ann Arbor, MI 48109, USA*

[c] *Abteilung für Membranbiochemie, Max-Planck-Institut für Biologie, 72076 Tübingen, Germany*

[d] *Department of Biochemistry and Biophysics, University of California San Francisco, 513 Parnassus Avenue, San Francisco, CA 94143, USA*

[e] *Abteilung für Parasitologie, Hygiene-Institut der Ruprecht-Karls-Universität, 69120 Heidelberg, Germany*

Received 8 June 2001; received in revised form 31 July 2001; accepted 21 August 2001

Abstract

Cysteine protease activity of African trypanosome parasites is a target for new chemotherapy using synthetic protease inhibitors. To support this effort and further characterize the enzyme, we expressed and purified rhodesain, the target protease of *Trypanosoma brucei rhodesiense* (MVAT4 strain), in reagent quantities from *Pichia pastoris*. Rhodesain was secreted as an active, mature protease. Site-directed mutagenesis of a cryptic glycosylation motif not previously identified allowed production of rhodesain suitable for crystallization. An invariable ER(A/V)FNAA motif in the pro-peptide sequence of rhodesain was identified as being unique to the genus *Trypanosoma*. Antibodies to rhodesain localized the protease in the lysosome and identified a 40-kDa protein in long slender forms of *T. b. rhodesiense* and all life-cycle stages of *T. b. brucei*. With the latter parasite, protease expression was five times greater in short stumpy trypanosomes than in the other stages. Radiolabeled active site-directed inhibitors identified brucipain as the major cysteine protease in *T. b. brucei*. Peptidomimetic vinyl sulfone and epoxide inhibitors designed to interact with the S_2, S_1 and S′ subsites of the active site cleft revealed differences between rhodesain and the related trypanosome protease cruzain. Using fluorogenic dipeptidyl substrates, rhodesain and cruzain had acid pH optima, but unlike some mammalian cathepsins retained significant activity and stability up to pH 8.0, consistent with a possible extracellular function. S_2 subsite mapping of rhodesain and cruzain with fluorogenic peptidyl substrates demonstrates that the presence of alanine rather than glutamate at S_2 prevents rhodesain from cleaving substrates in which P_2 is arginine.

Keywords: Rhodesain; Cathepsin; Trypanosome; Sleeping sickness; Recombinant expression

Abbreviations: BCIP, 5-bromo-4-chloro-3-indolyl-1-phosphate; CHN_2, diazomethane; DTT, dithiothreitol; E-64, *trans*-epoxysuccinyl-L-leucylamido-(4-guanidino)butane; HSMP-TBS-T, 5% horse serum and 1% milk powder in 10 mM Tris, 0.1 M NaCl, pH 8.0, 0.05% Tween 20; NBT, nitro blue tetrazolium; NMec, 7-amido-4-methylcoumarin; *N*-Me-pip, *N*-methyl-piperazine; PVDF, polyvinylidene difluoride; Rhodesain ΔC, rhodesain without the C-terminal extension; TLCK, tosyl lysyl chloromethyl ketone; VSPh, vinyl sulfone phenyl; YPD, yeast extract-peptone-dextrose; Z, benzyloxycarbonyl.

☆ *Note:* Nucleotide sequence data reported in this paper are available in the GenBank™, EMBL and DDBJ databases under the accession number AJ297265.

* Corresponding author. Tel.: +1-415-476-2940; fax: +1-415-750-6947.

E-mail address: jmck@socrates.ucsf.edu (J.H. McKerrow).

0166-6851/01/$ - see front matter
PII: S0166-6851(01)00368-1

1. Introduction

African trypanosomes are parasitic protozoa that afflict both man and animals. *Trypanosoma brucei gambiense* and *Trypanosoma brucei rhodesiense* are the causative agents of sleeping sickness in humans, and *Trypanosoma brucei brucei*, *Trypanosoma congolense* and *Trypanosoma vivax* are responsible for 'Nagana' in cattle. The parasites live extracellularly in blood and tissue fluids of their mammalian host and are transmitted by the bite of tsetse flies. Over 50 million people in 36 countries are at risk of acquiring the infection and 25 000–50 000 new cases are reported from 200 foci annually [1,2]. In addition, 46 million cattle are threatened with Nagana and losses to livestock producers and consumers cost approximately US$1340 million per year [3]. If left untreated, the disease in humans is fatal.

Current chemotherapy of human sleeping sickness is precarious [4]. Just four drugs are available, of which three (suramin, pentamidine and melarsopol) were developed over 50 years ago. Both suramin and pentamidine exhibit serious side effects and the latter is effective only against *T. b. gambiense* and not *T. b. rhodesiense*. With melarsopol, a serious reactive encephalopathy may result in 5–10% of patients treated with a 1–5% mortality. The sole new drug is eflornithine (DL-α-difluoromethylornithine, DFMO), a selective inhibitor of ornithine decarboxylase. First used in 1990, eflornithine is effective against *T. b. gambiense* but ineffective against *T. b. rhodesiense* [5]. Clearly, new strategies to treat sleeping sickness are required.

Cysteine proteases from a variety of protozoal parasites including *Plasmodium* spp. (malaria, [6]), *Trypanosoma cruzi* (Chagas' disease, [7]) and *Leishmania* spp. (leishmaniasis, [8]) have demonstrated potential as chemotherapeutic targets using peptidyl and peptidomimetic inhibitors [9]. In African trypanosomes, the major cysteine protease has a primary sequence and biochemical characteristics broadly similar to mammalian cathepsin L [10–12]. Recently, small-molecule inhibitors of this protease were shown to kill *T. b. brucei*, the model organism for human African trypanosomes, both in culture and experimentally infected animals [13–15]. Importantly, it was demonstrated that killing was correlated with inhibition of the cysteine protease brucipain [14]. Therefore, this protease and its orthologs in other African trypanosomes are attractive targets for chemotherapy based on cysteine protease inhibitors.

To implement a strategy of structure-based inhibitor design and inhibitor screening, reagent quantities of standardized protease are required. Therefore, we have expressed the *T. b. rhodesiense* cysteine protease rhodesain in *Pichia pastoris*. This is in preference to sourcing limiting amounts of possibly varying protease from the parasites themselves. We also describe a simple purification procedure and characterize the recombinant protease with respect to its physicochemical properties and sub-cellular localization. Finally, using peptidyl substrates and peptidomimetic inhibitors, we compare and contrast the active sites of recombinant rhodesain and cruzain.

2. Materials and methods

2.1. Design of rhodesain constructs for expression in *Pichia pastoris*

The cathepsin L-like cysteine proteases of trypanosomes [16,17] and *Leishmania* spp. [18] possess a characteristic C-terminal protein domain in addition to a catalytic domain. For this report, full-length *T. b. rhodesiense* rhodesain (including the C-terminal domain) and rhodesain without the C-terminal domain (ΔC) were expressed in *P. pastoris*. For both forms, that part of the gene encoding the pro-domain of the protease was included for expression as it was found previously for cathepsin L [19] and cruzain [20] that the pro-region is necessary for proper folding of the enzyme. Rhodesain was amplified by the polymerase chain reaction (PCR) from a unidirectional cDNA library of the *T. b. rhodesiense* strain MVAT4 (kindly provided by Dr John Donelson, University of Iowa, Iowa city) that had been constructed in Lambda Zap II (Stratagene, La Jolla, CA). PCR primers were: forward 5′-ATACTCGAGAAAAGAGCGTGCCTTGCGTCT-GT-3′ which incorporated an *Xho*I (Roche Molecular Biochemicals, Indianapolis, IN) site immediately 5′ of the *Pichia* Kex 2 endopeptidase recognition site (both sites are underlined); and reverse 5′-AATGCGGC-CGCTCACTGGTGTGGGACCAG-3′ for full length rhodesain, and 5′-AATGCGGCCGCTCAGGGGC-CTCCAACAACTGC-3′ for rhodesain ΔC (both reverse primers incorporated a transcription termination codon immediately 3′ of a *Not*I site and both are underlined). Amplification reactions (100 μl final volume) included 50 ng template, 10 mM Tris/HCl, pH 8.85, 25 mM potassium chloride, 5 mM ammonium sulfate, 2 mM magnesium sulfate, 0.2 mM dNTP, 100 pmol of each primer and 1.0 U Pwo polymerase (Roche). PCR was performed in a Perkin Elmer Thermal Cycler with 35 cycles of 94, 55 and 72 °C, each for 1 min. PCR products were resolved in 1% agarose gels containing 0.5 μg ml^{-1} ethidium bromide, and purified from the agarose (Qiagen, Valencia, CA). Purified DNA was restriction digested overnight at 37 °C with *Xho*I and *Not*I, re-purified and then ligated into the expression vector pPIC Zα A (Invitrogen Corp., San Diego, CA) which had been similarly digested with the same enzymes and purified. The resulting construct places the rhodesain gene 3′ of the

α-mating factor of *P. pastoris*, thereby targeting rhodesain for secretion. Sufficient recombinant plasmid was produced in and purified from *Escherichia coli* (DH5α strain; Life Technologies, Rockville, MD) for sequencing and electroporation of *P. pastoris* (see below). The entire pro-mature-C-terminus of rhodesain was sequenced in both directions (Sequetech Corp., Mountain View, CA). To obtain the sequence encoding the N-terminal signal peptide of rhodesain, the protease gene was amplified from the Lambda Zap II library by PCR as described above using the forward primer 5′-ATGATGCTATTCTCTTTATTTCTTA-3′ (based on the previous rhodesain sequence accession CAA38238 [21]) and the rhodesain ΔC reverse primer. The amplified product was sequenced in both directions (Sequetech).

2.2. Site-directed mutagenesis

To produce rhodesain for crystallography, the previously unidentified glycosylation site at Asn^{295} of rhodesain ΔC (see Section 3) was mutated to alanine by site-directed mutagenesis using sequential PCR steps [22]. PCR was as described above and incorporated the mutation primer 5′-GTTGGTTACAATGATGCTAGCAATCCACCC-3′ or its anti-parallel counterpart (bases encoding the mutation are underlined), the appropriate forward or reverse primer and 5 ng of rhodesain ΔC–pPIC Zα A plasmid as template. The mutation primers used introduced a unique *Nhe*I restriction site to monitor the success of the mutation.

2.3. Expression of rhodesain in Pichia pastoris

Procedures to express rhodesain in *P. pastoris* were modified from those detailed by the manufacturer (Invitrogen). Briefly, to allow for homologous incorporation of the recombinant plasmid into the *AOX 1* locus of the *Pichia* genome, recombinant pPIC Zα A (10 μg) was linearized with *Sac*I and purified. The X33 strain of *P. pastoris* (Invitrogen) was electroporated at 1.5 kV and 129 Ω in electroporation cuvettes (2 mm gap; BTX, San Diego, CA). *Pichia* colonies growing at 30 °C under zeocin (100 μg ml^{-1}; Invitrogen)—selection on yeast extract-peptone-dextrose (YPD) agar plates were picked for expansion first in 10 ml and then in 500–1000 ml of YPD medium containing the same concentration of antibiotic. Expression of recombinant protein was induced by incubating transformed *Pichia* for 24–48 h at 30 °C in buffered minimal medium (200–400 ml) containing 1% methanol as the sole carbon source. Protease activity in the medium was monitored by hydrolysis of the fluorogenic peptidyl substrate benzyloxycarbonyl-phenylalanyl-arginine-7-amido-4-methylcoumarin (Z-Phe-Arg-NMec; see below).

2.4. Purification of recombinant rhodesain

Pichia culture supernatants containing rhodesain were lyophilized and stored in a desiccator at 4 °C until use. Lyophilized samples were resuspended in 10% of the original volume in 0.05 M sodium acetate, pH 5.5 and complete equilibration with this buffer was accomplished using PD10 columns (Amersham Pharmacia Biotech, Piscataway, NJ). The solution was concentrated 10-fold in Centricon-10 ultrafiltration units (10 kDa cutoff; Millipore, Bedford, MA), adjusted to pH 4.5 with 4 M sodium acetate, pH 4.5, and left overnight at 37 °C in the presence of 2 mM dithiothreitol (DTT) to allow the protease activity to 'clear' the solution of any incompletely processed forms of rhodesain and contaminating proteins. Finally, PD10 columns equilibrated with 0.05 M sodium acetate, pH 5.5 were used to remove DTT and exchange the buffer for storage of rhodesain at −80 °C until use.

2.5. SDS-PAGE, N-terminal sequencing and glycosylation status of recombinant rhodesain

Purification of rhodesain was monitored by sodium dodecyl sulphate-polyacrylamide gel electrophoresis (SDS-PAGE) [23] through 4–12% gradient gels (Invitrogen). Gels were stained in 40% methanol, 10% acetic acid containing 0.5% Coomassie Brilliant Blue R-250 (BIO-RAD, Hercules, CA) and destained in the same solution without Coomassie. For N-terminal sequencing, samples were subjected to SDS-PAGE and transferred to polyvinylidene difluoride (PVDF) membranes (Immobilon-P, Millipore) for 45 min at 25 V using the procedures and apparatus supplied by Invitrogen. Bands were visualized in 0.1% Ponceau S (Sigma, St. Louis, MO), excised and destained in water. Sequencing was performed by the UCSF Biomolecular Resource Facility using the Edman degradation technique.

To determine the glycosylation status of recombinant rhodesain, purified enzyme (40 μg as measured by the BCA reagent; Pierce Rockford, IL) was incubated with PNGase F according to the procedures described by New England Biolabs, Beverly, MA (product number 704S). Briefly, sample was reduced and boiled for 10 min in 5% SDS and 10% β-mercaptoethanol. One-tenth volumes of 0.5 M sodium phosphate, pH 7.5 and 10% NP-40 were then added and the solution incubated with 500 U PNGase F for 4 h at 37 °C. Samples were separated by SDS-PAGE and stained as described above.

2.6. Production of antisera to rhodesain

Antisera to full length rhodesain and rhodesain ΔC were raised in New Zealand white rabbits by Covance, Richmond, CA. Prior to each injection protocol, preim-

mune serum was collected and stored at −20 °C. Each injection used PNGase F-treated rhodesain (200 μg) that had been excised from SDS-polyacrylamide gels and mixed with an equal volume (200 μl) of adjuvant. Freund's complete adjuvant was used for the primary injection (day 1), whereas Freund's incomplete adjuvant was used for the second and third injections on days 18 and 36, respectively. Rabbits were exsanguinated at 54 days and sera stored at −20°C.

2.7. Cultivation of T. b. brucei and T. b. rhodesiense

Bloodstream forms of the pleomorphic *T. b. brucei* variant clone AnTat 1.1 [24] were grown in NMRI mice. Dividing long slender and cell-cycle arrested short stumpy trypanosomes were purified from blood by DEAE–cellulose chromatography [25] 3 and 5 days post-infection, respectively. Procyclic insect forms of *T. b. brucei* AnTat 1.1 were cultivated at 27 °C in SDM-79 medium [26] supplemented with 10% heat-inactivated fetal bovine serum. Bloodstream forms of the monomorphic *T. b. rhodesiense* clone STIB 704 [27] were grown under a humidified atmosphere at 37 °C containing 5% CO_2 in HMI-9 medium [28], supplemented with 16.7% heat-inactivated fetal bovine serum.

2.8. Immunoblotting

Pure full length rhodesain and rhodesain ΔC (5 μg) were resolved by SDS-PAGE (4–12% gradient gels) and transferred to PVDF membrane as described above. For parasite extracts of long slender, short stumpy and procyclic *T. b. brucei*, and long slender *T. b. rhodesiense*, 6×10^7 per ml cells were lysed on ice in 50 mM Na–Hepes, 2.5 mM ethylenediaminettetraacetic acid (EDTA), 2 mM EGTA, pH 7.0 supplemented with protease inhibitors (200 μM tosyl lysyl chloromethyl ketone (TLCK), 400 μM PMSF, 10 μM leupeptin, 2 μM *trans*-epoxysuccinyl-L-leucylamido-(4-guanidino)-butane (E-64) and 1 μM pepstatin A) until no intact parasites could be seen microscopically. Each parasite extract (2 μg) was subjected to SDS-PAGE (10% gels) and transferred to PVDF. Following blocking of the membrane overnight in 10 mM Tris, 0.1 M NaCl, pH 8.0, 0.05% Tween 20 (TBS-T) containing 5% horse serum and 1% milk powder (HSMP), the membrane was incubated with preimmune, anti-full length rhodesain or anti-rhodesain ΔC serum at a dilution of 1/4000 (pure rhodesain) or 1/1000 (parasite extracts) in HSMP-TBS-T for 60 min. The membrane was then washed 5×5 min in TBS-T and incubated for 1 h in HSMP-TBS-T containing either alkaline phosphatase-conjugated goat anti-rabbit IgG diluted 1/4000 (2.5 μg; Life Technologies) for pure rhodesain or horseradish peroxidase-conjugated goat anti-rabbit IgG diluted 1/5000 (4 μg; Santa Cruz Biotechnology, Santa Cruz, CA) for parasite extracts. After the same washing steps, blots with pure rhodesain were developed in 0.1 M Tris/HCl, 0.1 M NaCl, 5 mM $MgCl_2$, pH 9.0 containing 0.33% nitro blue tetrazolium (NBT; Promega, Madison, WI) and 0.66% 5-bromo-4-chloro-3-indolyl-1-phosphate (BCIP; Promega). Development was stopped by incubating the membrane in TBS containing 5 mM EDTA. For development of blots with parasite extracts, the ECL kit was employed as described by the manufacturer (Amersham Pharmacia Biotech). Band intensities as developed by ECL were quantified by densitometry using the software NIH Image Version 1.62.

2.9. Radiolabeling of cysteine protease activity in trypanosome extracts

Extracts of bloodstream-form pleomorphic *T. b. brucei* variant clone AnTat 1.1 were prepared as described above for the immunoblotting experiments, but in the absence of the protease inhibitor cocktail. Labeling experiments were performed essentially as previously described [29]. Lysates (100 μg protein) were added to reaction buffer (50 mM Tris, pH 5.5, 5 mM $MgCl_2$, 2 mM DTT) in a final volume of 100 μl. Radiolabeled morpholinourea-leucinyl-homophenylalanine vinyl sulfone phenol (^{125}I-LHVS-PhOH; approximately 10^6 cpm per sample) was added and samples incubated on ice for 2 h. To determine whether the reaction of the radiolabeled vinyl sulfone with the protease target was specific, lysates were preincubated for 30 min at room temperature with 10 μM of the selective cysteine protease inhibitors benzyloxycarbonyl-phenylalanyl-alanine diazomethane (Z-Phe-Ala-CHN_2; Bachem, Torrance, CA) or *N*-methyl-piperazine-phenylalanyl-homophenylalanine-vinyl sulfone phenyl (*N*-Me-pip-Phe-homoPhe-VSPh; kindly given by Dr James Palmer, Axys Pharmaceuticals, South San Francisco, CA) prior to addition of the radiolabeled inhibitor. The labeling reaction was quenched by addition of 4× SDS sample buffer followed by boiling. Labeling profiles were obtained by separation of protein by SDS-PAGE (12.5% gels) followed by autoradiography [30].

2.10. Immunoelectron microscopy

Bloodstream forms of *T. b. rhodesiense* clone STIB 704 were fixed with 2% formaldehyde/0.05% glutaraldehyde in phosphate buffered saline (PBS), and infiltrated with a mixture of 20% polyvinylpyrrolidon/1.8 M sucrose [31]. Ultrathin cryosections were blocked with 1% skimmed milk/0.5% bovine serum albumin (BSA) in PBS, incubated with anti-rhodesain ΔC rabbit serum (1:50)/protein A-15 nm gold or preimmune serum (1:50)/protein A-15 nm gold as previously described

[32]. For double-labeling, anti-rhodesain ΔC/protein A-15 nm gold-labeled cells were fixed with 0.5% glutaraldehyde for 10 min and then incubated with mouse monoclonal IgM (1/200 dilution) to the *T. b. brucei* lysosomal glycoprotein CB1 ([33] Cedarlane, Hornby, Ont., Canada) and goat anti-mouse IgM IgG-10 nm gold (Aurion, Wageningen, The Netherlands). Final uranylacetate staining and methyl cellulose embedding were performed as described [34].

2.11. Measurement of rhodesain activity with NMec substrates

For comparison with rhodesain, many of the studies involving 7-amido-4-methylcoumarin (NMec) substrates included the orthologous enzyme cruzain (2 nM) from *T. cruzi* (produced recombinantly according to [20] and minus the C-terminal domain). The standard assay used Z-Phe-Arg-NMec and initial rates of activity were measured at room temperature in black 96-well microtiter plates (Corning, Corning, NY) using a Labsystems Fluoroskan II fluorometer at excitation and emission wavelengths of 350 and 460 nm, respectively. Full length rhodesain or rhodesain ΔC (2 nM) was preincubated for 5 min in 100 μl 0.1 M sodium acetate, pH 5.5, containing 2 mM DTT. Substrate (100 μl; 20 μM), in the same buffer, was added and the reaction continued for 5 min. For determination of the Michaelis constant, K_m, a range of substrate concentrations between 0.1 and 40 μM was employed and the value estimated graphically [35]. The concentration of active enzyme used in assays was determined by active site titration with E-64, a stoichiometric irreversible inhibitor of papain-like cysteine proteases [36]. Experiments were also performed with rhodesain ΔC to compare the initial rates of hydrolysis of Z-Leu-Arg-NMec, Z-Val-Arg-NMec (kindly provided by Dr Dieter Brömme, Mount Sinai School of Medicine, New York) and Z-Arg-Arg-NMec (Bachem), with that of Z-Phe-Arg-NMec. For these tests, the effect of pH on the hydrolysis of a given substrate was measured at pH 4.0, 5.0, 6.0 and 7.0 as described below.

2.12. pH activity and stability of rhodesain

A citrate–phosphate buffer (0.1 M) was used to obtain initial rates of activity over the pH range of 3.0–8.0. Results were compared with cruzain. All buffers contained 0.3 M NaCl to minimize variations in ionic strength. The pH stability of full length rhodesain, rhodesain ΔC and cruzain was determined by incubating the protease at 37 °C in 0.1 M sodium acetate, pH 5.5 (representing lysosomal pH) and 0.1 M sodium phosphate, pH 7.3 (cytosolic and extracellular pH) without DTT. At various times up to 3 h, aliquots were withdrawn and activity measured with Z-Phe-Arg-NMec as described above.

2.13. Effects of vinyl sulfone and epoxide inhibitors

The C-terminal domain of rhodesain, like that of its ortholog, cruzain, does not contribute to the catalysis of small synthetic substrates (see Section 3). Therefore, experiments with small-molecule inhibitors utilized rhodesain ΔC for comparison with recombinant cruzain (also ΔC). Reactions were performed as described [37] at pH 5.5 with Z-Phe-Arg-NMec under the conditions detailed above. The time-dependent inhibition of rhodesain ΔC and cruzain was analyzed using progress curves in the presence and absence of inhibitor. Reactions were started by addition of enzyme to solutions of substrate and inhibitor. Values for the pseudo-first-order rate constant k_{obs} at each concentration of inhibitor $[I]_o$ were computed for individual curves by fitting the data to Eq. (1) when $[I]_o \geq 10$ times the enzyme concentration $[E]_o$, where $[P]$ is the concentration of product formed over time t, and v_0 is the initial velocity of the reaction.

$$[P] = \frac{v_0}{k_{obs}}(1 - \exp^{-k_{obs}t}) \quad (1)$$

If k_{obs} varied linearly with $[I]_o$, then the association constant k_{ass} was determined by linear regression analysis using Eq. (2).

$$k_{obs} = \frac{k_{ass}[I]_o}{(1 + [S]_o/K_m)} \quad (2)$$

where $[S]_o$ is the concentration of substrate.

If k_{obs} varied hyperbolically with $[I]_o$, then non-linear regression analysis was performed to determine the inactivation constant k_{inact} and the inhibition constant K_i using Eq. (3).

$$k_{obs} = \frac{k_{intact}[I]_o}{([I]_o + K_i{*}(1 + [S]_o/K_m))} \quad (3)$$

where $K_i{*} = K_i(1 + [S]_o/K_m)$.

2.14. Homology-based modeling of rhodesain on cruzain

A model structure of rhodesain ΔC was constructed using the 1.6 Å structure of cruzain bound to a peptidomimetic vinyl sulfone inhibitor (PDB ID: 1F2A) [38] and the 2.8 Å structure of papain (PDB ID: 1PAD) as 3-D templates of related fold. Homology models of rhodesain were generated with MODELER [39], a module of the Quanta software package (MSI). Quanta was used for visualization and comparison of generated models.

3. Results and discussion

3.1. Production of pure, active recombinant rhodesain

Full length rhodesain and rhodesain ΔC were secreted as active enzymes from *P. pastoris*. Also, the deglycosylated rhodesain ΔC generated by site-directed mutagenesis was active. Proteolysis was monitored with the peptidyl fluorogenic substrate Z-Phe-Arg-NMec. Purification of the various rhodesain preparations from induced *P. pastoris* culture supernatants (Fig. 1A, B and C, lane 1) was relatively simple involving a convenient lyophilization step, a 'clearing' step at acid pH (to remove any remaining enzyme proforms and protein contaminants), and buffer exchanges. A similar clearing procedure has been used to remove contaminants for purification of orthologous cysteine proteases [40]. Upon clearing, two protein species were visualized by SDS-PAGE for full length rhodesain (Fig. 1A, lane 2) and rhodesain ΔC (Fig. 1B, lane 2), resolving at 36 and 34 kDa, and 27 and 24 kDa, respectively. A single band at 25 kDa was resolved for the deglycosylated mutant ($Asn^{295} \rightarrow Ala$) of rhodesain ΔC (Fig. 1C, lane 2).

For all purified protein bands, the N-terminal amino acid sequences were identical (T G R A P), thus indicating that all but three of the pro-domain amino acids had been removed (see [21] for sequence of rhodesain). These bands, representing mature rhodesain, are the major proteins secreted by transformed *P. pastoris*. The secretion of mature fully active rhodesain contrasts with the production of cathepsins F [41] and V [42], which were produced as pro-enzymes in the same expression system. For those enzymes, auto-activation at acid pH was necessary to convert the pro-cathepsins to their mature active forms.

The presence of two bands for full length rhodesain and rhodesain ΔC is consistent with the modification of one or more glycosylation sites. Treatment with the *N*-glycosidase PNGase F prior to electrophoresis eliminated the upper band in full length rhodesain (Fig. 1A, lane 3). Similar results were obtained with rhodesain ΔC (not shown). The difference in molecular mass between full length rhodesain and rhodesain ΔC (approximately 10 kDa) is consistent with the theoretical value of 11.1 kDa for the C-terminal domain.

Final protein yields of purified rhodesain ΔC and its deglycosylated variant were in the range of 40–60 mg l^{-1} of induced *Pichia* culture, whereas those of full length rhodesain were in the range of 20–40 mg l^{-1}. Active site titration experiments with the irreversible peptidyl epoxide inhibitor E-64 indicated that 50–75% of each purified rhodesain preparation was folded prop-

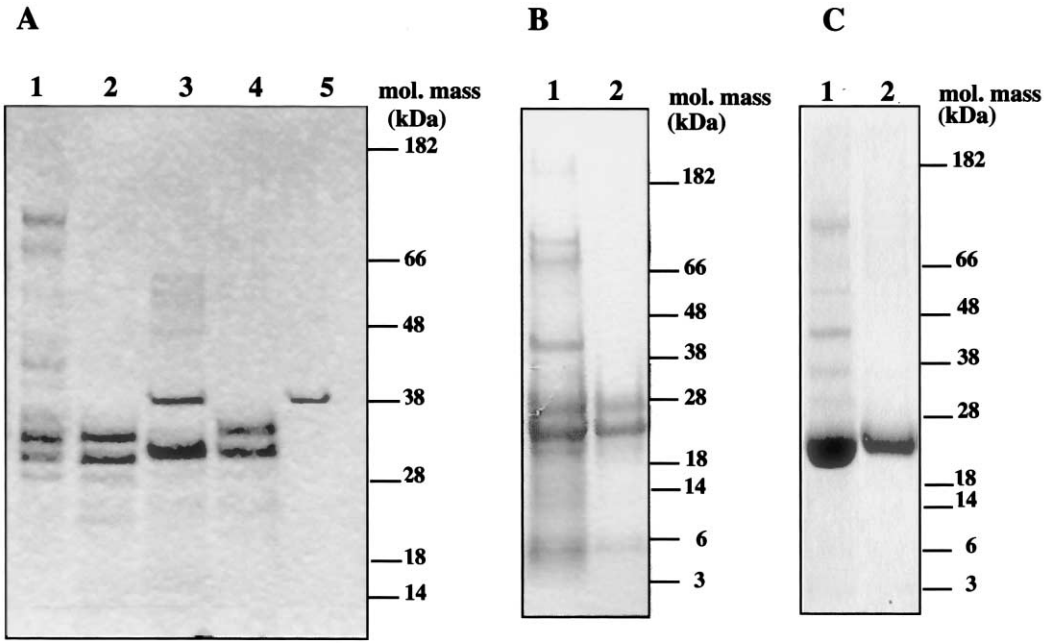

Fig. 1. Purification of full length rhodesain, rhodesain ΔC and the deglycosylated mutant ($Asn^{295} \rightarrow Ala$) of rhodesain ΔC. (A) concentrated induction medium and fractions thereof from *P. pastoris* transformed with pPIC Zα A-full length rhodesain were prepared as described in the text and subjected to SDS-PAGE in a 4–12% gradient gel (30 μg protein load). Lane 1, concentrated induction medium; lane 2, concentrated medium allowed to clear overnight at 37 °C; lane 3, cleared medium incubated with PNGase F; lane 4, as for lane 3 but without PNGase F; lane 5, as for lane 3 but without rhodesain. (B) as described for (A) but using *P. pastoris* transformed with pPIC Zα A-rhodesain ΔC (30 μg protein load). Lane 1, concentrated induction medium; lane 2, concentrated medium allowed to clear overnight at 37 °C. (C) as described for (A) but using *P. pastoris* transformed with the deglycosylated mutant ($Asn^{295} \rightarrow Ala$) of rhodesain ΔC (40 μg protein load). Lane 1, concentrated induction medium; lane 2, concentrated medium allowed to clear overnight at 37 °C. Gels were stained with Coomassie Blue R-250. For (A), (B) and (C), molecular masses in kDa are indicated on the right.

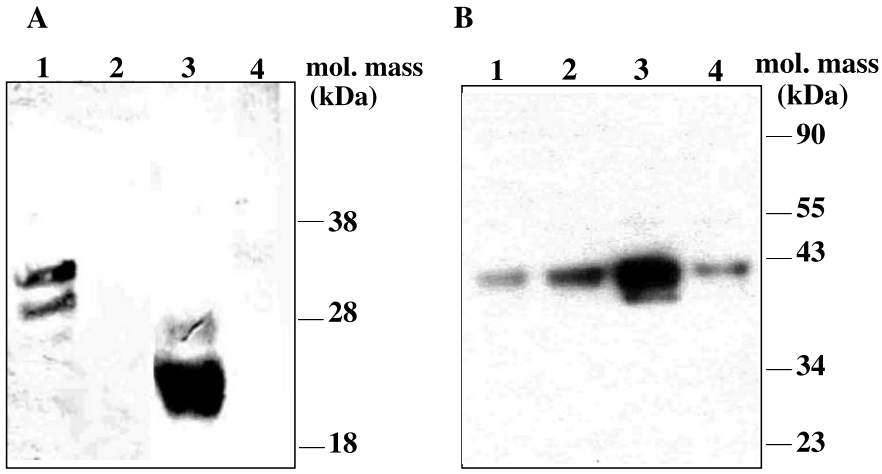

Fig. 2. Immunoblotting of recombinant rhodesain and lysates of life cycle stages of *T. b. rhodesiense* and *T. b. brucei*. (A) Pure recombinant full length rhodesain and rhodesain ΔC (5 μg of each) were subjected to SDS-PAGE (4–12% gels), blotted onto PVDF and probed with their respective rabbit anti-sera. Alkaline phosphatase-conjugated goat anti-rabbit IgG was used as secondary antibody and the blot was developed with BCIP/NBT solution. Lanes 1 and 3, full length rhodesain and rhodesain ΔC probed with their respective hyperimmune sera, and, lanes 2 and 4, probed with pre-immune sera. Molecular masses in kDa are indicated on the right. (B) Extracts (2 μg) of various life cycle stages of *T. b. rhodesiense* and *T. b. brucei* were subjected to SDS-PAGE (10% gel), blotted to PVDF and reacted with rabbit anti-rhodesain ΔC serum. The secondary antibody was horseradish peroxidase-conjugated goat anti-rabbit IgG and the blot was developed with the ECL reagent. Lane 1, extracts of *T. b. rhodesiense* long slender forms; lanes 2–4, extracts of *T. b. brucei* long slender, short stumpy and procyclic forms. Molecular masses in kDa are indicated on the right. The result shown is one of a total of three experiments performed yielding identical results.

erly and active on a protein-weight basis. The simplicity of the preparation of pure rhodesain using *P. pastoris* is a significant improvement over the use of *E. coli* as an expression system [43]. In that system, rhodesain was sequestered in insoluble inclusion bodies, processed heterogeneously, and only partially renaturable.

3.2. Sequence analyses of rhodesain and identification of a novel pro-peptide motif

Initial attempts to produce non-glycosylated rhodesain ΔC for crystallography failed and a doublet banding pattern was visualized on SDS gels (Fig. 1B, lane 2). We, therefore, sequenced the entire 1350 bp open reading frame (ORF) of full length rhodesain in both directions to identify a possible cryptic glycosylation site. Such was found at Asn^{295} (numbering system as reported for sequence accession CAA38238, [21]). The different strains of *T. b. rhodesiense* used here (MVAT4) and previously (WRATat 1.1, [21]) as sources of DNA most likely explain the presence of this unique site. The site-directed mutation $Asn^{295} \rightarrow Ala$ successfully eliminated this glycosylation site as judged by SDS-PAGE (compare lane 2 in Fig. 1B and C). Complete examination of the present sequence identified a total of 12 nucleotide changes from that reported previously. Nine of these are silent. There are three amino acid changes; Leu^{115} for Val, Ser^{297} for Asn, and Leu^{412} for Pro. Otherwise, the primary sequences of rhodesain from both strains are identical and share two potential glycosylation sites, one in the pro-region (Asn^{120}) and the other in the C-terminal domain (Asn^{397}).

Rhodesain and its orthologs from *T. b. brucei* ([16], CAA34485), *T. congolense* ([44], CAA30181), *T. rangeli* ([45], AAA79289) and *T. cruzi* ([20], AAA30181) possess an ER(A/V)FNAA motif (EX_3RX_2(A/V)(F/W)$X_2NX_3AX_3$A) in the pro-peptide which does not vary and is apparently unique to the genus *Trypanosoma*. The motif is analogous to the ER(I/V)FNAQ and ER(I/V)FNIN motifs of the mammalian cathepsin F/W [46], and cathepsin L groups [47], respectively. Components of this motif function to stabilize the interaction of the second α-helix with that of a subsequent β-sheet in the pro-domain [48]. The corresponding motif (ER(V/N/A)(F/S)N(A/M)(N/Q) of the orthologous *Leishmania* cysteine proteases from *Leishmania major* ([18], AAB48120), *Leishmania mexicana* ([49], CAA44094; [50], CAA90237) and *Leishmania donovani* ([51], AAC38833) differs from that of the trypanosomes and exhibits considerable variability within the genus. The separation of *Trypanosoma* and *Leishmania* described above accords with their separate placements in dendograms constructed using distance and parsimony analyses based on the sequences of either cathepsin L-like proteases or ribosomal RNA genes [18].

3.3. Identification of rhodesain/brucipain in trypanosome life cycle stages

Rabbit hyperimmune antisera to full length rhodesain and rhodesain ΔC reacted with their respective target recombinant proteins (Fig. 2A, lanes 1 and 3). Pre-immune sera did not react (Fig. 2A, lanes 2 and 4). When tested with extracts of the different life-cycle stages of trypanosomes, antiserum to rhodesain ΔC reacted with a major 40 kDa protein in bloodstream forms of *T. b. rhodesiense* (Fig. 2B, lane 1), and in long slender, short stumpy and procyclic forms of *T. b. brucei* (Fig. 2B, lanes 2–4, respectively). Cross-reactivity of the anti-rhodesain ΔC serum with the ortholog brucipain in *T. b. brucei* was not unexpected given that the proteases share 98.4% identity in amino acid sequence. By scanning densitometry, the reaction of the antiserum with protease in extracts of the short stumpy stage was approximately 5-fold stronger than in either of the long slender or procyclic stages, thus suggesting that short stumpies contain more brucipain. This observation is consistent with the demonstration using fluorogenic substrates that short stumpies of *T. b. rhodesiense* [52] and *T. b. brucei* [53] contain higher cysteine protease activities than either long slenders or procyclics. The higher levels of protease activity in the short stumpy stage might be associated with the protein and cellular reorganization necessary to prepare the parasite for survival in the tsetse fly. Using anti-rhodesain ΔC serum, a major 40 kDa band was also identified by immunoblotting extracts of *T. b. evansi*, a mechanically transmitted trypanosome of horses and wildlife in central Asia and South America (M. Gonzatti, personal communication).

3.4. Identification of rhodesain/brucipain as the major trypanosome cysteine protease

The identification of a 40 kDa cysteine protease in trypanosome extracts was confirmed by use of the radiolabeled, active site-directed inhibitor ^{125}I-LHVS-PhOH (Fig. 3, lane 1). This band was the major reacting protease species. The reaction could be inhibited by prior incubation of extracts with the known trypanosome cysteine protease inhibitors Z-Phe-Ala-CHN_2 and *N*-Me-pip-Phe-homoPhe-VSPh (Fig. 3, lanes 2 and 3). Fainter labeled proteases at 33 and 29 kDa were also visualized and may represent differentially glycosylated forms of brucipain lacking the C-terminal domain, or other minor cysteine proteases. Together, the results of the immunoblotting and active-site labeling experiments demonstrate that rhodesain/brucipain is the predominant cysteine protease activity of 40 kDa in *T. b. rhodesiense* and *T. b. brucei*. The 40 kDa value is consistent with the mature glycosylated protease bound to its C-terminal domain.

3.5. Localization of rhodesain in the lysosome

Heretofore, only indirect evidence has suggested that the major cysteine protease of *T. brucei* was localized in the lysosome as judged by the detection of proteolytic activity associated with cellular fractions containing lysosome-like organelles [10]. Here, immunoelectron microscopy of *T. b. rhodesiense* bloodstream forms with anti-rhodesain ΔC serum directly demonstrates that the protease is localized in the lysosome (Fig. 4A). Preimmune serum did not react (Fig. 4C). Rhodesain co-localizes with the major lysosomal glycoprotein CB1, a lysosomal marker of *T. brucei* ([33], Fig. 4B). The same pattern of labeling was observed with sections of *T. b. brucei* bloodstream forms (not shown). The localization of rhodesain in the lysosome is consistent with the previous demonstration that incubation of trypanosomes with the cysteine protease inhibitor Z-Phe-Ala-CHN_2 leads to an accumulation of undegraded protein in that organelle [14]. As the major proteolytic activity in the lysosome, rhodesain is likely to be involved in the degradation of parasite proteins and

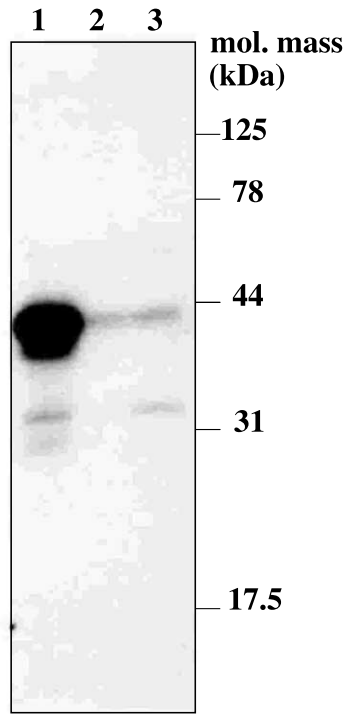

Fig. 3. Active site radiolabeling of brucipain in extracts of *T. b. brucei*. Cell extracts (100 μg) of *T. b. brucei* were incubated with the radiolabeled cysteine protease inhibitor ^{125}I-LHVS-PhOH and subjected to SDS-PAGE (12.5% gel) followed by autoradiography. Lane 1, extracts incubated with the radiolabel without prior inhibition with non-labeled inhibitor; lanes 2 and 3, extracts pre-incubated with the selective cysteine protease inhibitors Z-Phe-Ala-CHN_2 and *N*-Me-pip-Phe-homoPhe-VSPh, respectively, prior to addition of ^{125}I-LHVS-PhOH. Note the almost complete blocking of binding of ^{125}I-LHVS-PhOH by preincubation with the non-labeled inhibitors. Molecular masses in kDa are indicated on the right.

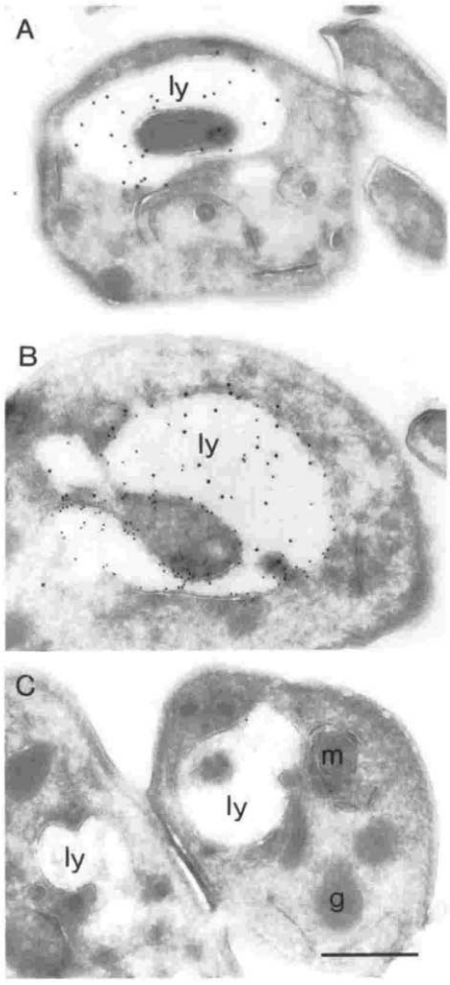

Fig. 4. Ultrathin cryosection immunogold labeling of rhodesain in *T. b. rhodesiense* bloodstream forms. (A) Cross-section that was labeled with anti-rhodesain ΔC rabbit serum and protein A-15 nm gold. (B) Cross-section that was double-labeled with both anti-rhodesain ΔC rabbit serum/protein A-15 nm gold and mouse monoclonal antibodies to the *T. b. brucei* lysosomal glycoprotein CB1/anti-mouse IgM-10 nm gold. (C) Cross-section that was labeled with preimmune serum and protein A-15 nm gold. ly, Lysosome; g, glycosome; m, mitochondrion. Bar, 0.5 μm.

intracellularly transported host proteins in both the insect and the mammalian host. A function for the orthologous enzyme, congopain, in the degradation of variant surface glycoprotein in the lysosome has been discussed [54].

3.6. pH profile and stability of rhodesain compared with cruzain

At optimal pH with Z-Phe-Arg-NMec as substrate, full length rhodesain and rhodesain ΔC had K_m values of 1.2 ± 0.3 and 1.5 ± 0.4 μM, respectively (means ± S.D. values from three separate experiments). For cruzain, a K_m value of 0.96 ± 0.049 μM had been determined previously [20]. The pH profiles of all three enzymes were similar with maximal activity against Z-Phe-Arg-NMec between pH 5.0 and 5.5 (Fig. 5A). Therefore, the presence of the C-terminal domain of rhodesain seems not to influence the pH activity of the enzyme. The acid pH optima of rhodesain and cruzain are consistent with their lysosomal localization and similar to the pH optima of mammalian cathepsins,

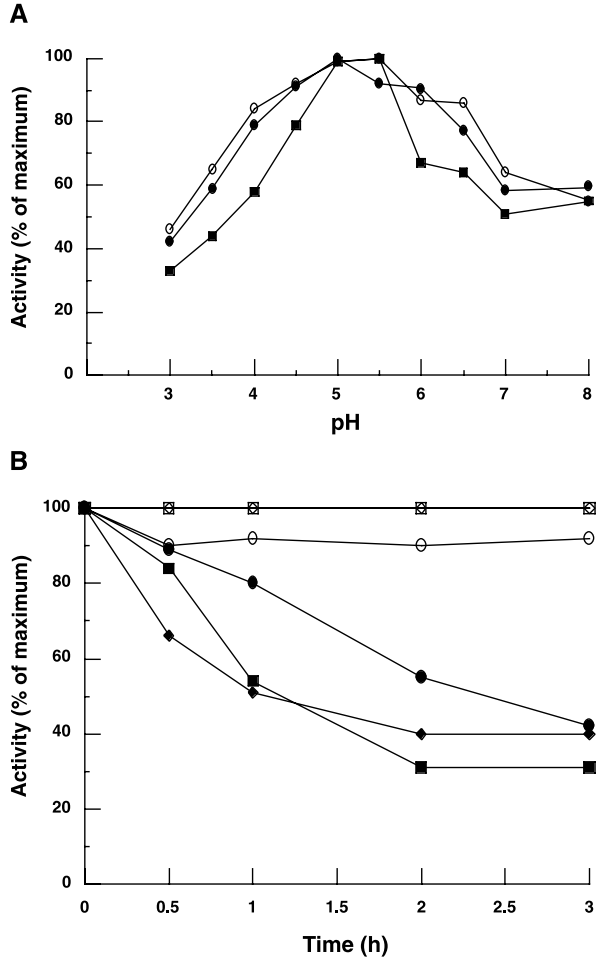

Fig. 5. pH dependent activities and stabilities of full length rhodesain, rhodesain ΔC and cruzain with Z-Phe-Arg-NMec as substrate. (A) For pH profiles, each protease was preincubated in 0.1 M citrate-phosphate, 0.3 M NaCl, 2 mM DTT. Then, the same volume of buffer containing Z-Phe-Arg-NMec (20 μM) was added. Activity was measured at room temperature by fluorescence emission at 460 nm (●, full length rhodesain; ■, rhodesain ΔC; ○, cruzain). For each protease, activities were compared with the maximum, which was set to 100%. (B) For pH stability experiments, each protease was incubated at 37 °C in either 0.1 M sodium acetate, pH 5.5 (to simulate the lysosomal pH) or 0.1 M sodium phosphate, pH 7.3 (cytosolic and extracellular pH) for up to 3 h. At the times indicated, aliquots were removed and activity measured at room temperature with 10 μM Z-Phe-Arg-NMec by fluorescence emission at 460 nm. At pH 5.5, □, full length rhodesain; ◇, rhodesain ΔC; ○, cruzain. At pH 7.2, ■, full length rhodesain; ◆, rhodesain ΔC; ●, cruzain. For both A and B, experiments were performed in triplicate and S.D. values were never greater than 5% of the mean.

such as cathepsins F [41], V [42] and L [55]. However, unlike some mammalian cathepsins, such as cathepsin F and L, which are inactivated quickly at pH values at and above 7.0, the trypanosome proteases retained significant activity (> 50% of original at pH 8.0). Similarly, brucipain, purified from *T. b. brucei* extracts, has been shown to maintain significant activity up to pH 9.0 [12].

In addition, pH stability experiments demonstrated that full length rhodesain, rhodesain ΔC and cruzain are stable at the cytosolic and extracellular pH of 7.3 (Fig. 5B). All enzymes displayed only a slow loss of activity over 3 h, at which time greater than 30% of original activity remained. The activity and stability of rhodesain at neutral pH is interesting given the report that cysteine protease activity is secreted by living intact *T. b. brucei* in culture [56]. If secreted into the infected host, it might be expected that rhodesain would be inhibited by serum protease inhibitors such as the kininogens and α_2-macroglobulin, as has been reported in vitro for brucipain [12]. Nevertheless, brucipain has been shown to form active complexes with L-kininogen [57] and it is possible for rhodesain that such circulating complexes and/or the retention of proteolytic activity may confer some advantage to the parasite by modulating host physiology or the immune response.

3.7. S_2 subsite specificity of rhodesain compared with cruzain

For papain-like cysteine proteases, such as rhodesain, the S_2 subsite (in the nomenclature of Schechter and Berger [58]) of the active site cleft defines the primary specificity towards peptidyl substrates. The S_2 specificity of rhodesain ΔC (Fig. 6A) was compared with that of cruzain (Fig. 6B) using four dipeptidyl fluorogenic substrates in which the P_2 amino acid was varied (Phe, Leu, Val or Arg). Analyses were conducted at pH 4.0, 5.0, 6.0 and 7.0. Consistent with the preference of many mammalian cysteine-class cathepsins [41,42], both trypanosome enzymes prefer bulky hydrophobic amino acids in S_2. Rhodesain has an equal preference for leucine and phenylalanine whereas cruzain prefers phenylalanine. Both enzymes are approximately 50% less reactive with the substrate containing a β-branched valine. Taken together, rhodesain resembles more cathepsin F in its S_2 specificity, whereas cruzain is more similar to cathepsin L [42]. The major difference between the rhodesain and cruzain was in their respective abilities to degrade the substrate with arginine at P_2. The presence of glutamate at the base of the S_2 subsite (Glu^{333} (Glu^{205} in papain numbering)) in cruzain would allow interaction with the positively charged arginine side chain [59], whereas the corresponding alanine in rhodesain would not have such an attraction.

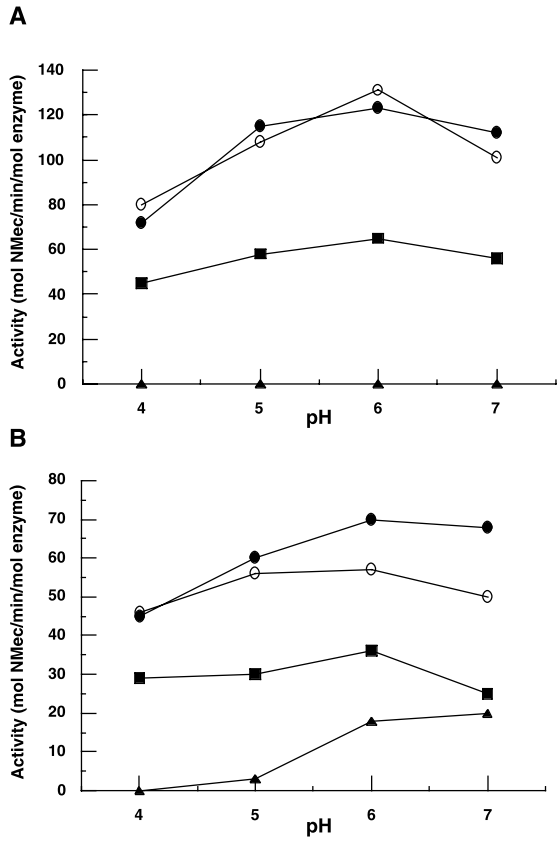

Fig. 6. Specificity of the S_2 subsite of rhodesain ΔC compared with cruzain. Each protease was tested at four pH values with four substrates (10 μM) varying at the P_2 position (Z-Xxx-Arg-NMec, where Xxx indicates phenylalanine (●), leucine (○), valine (■), or arginine (◆). Activity was measured at room temperature by fluorescence emission at 460 nm. (A) and (B), data for rhodesain ΔC and cruzain, respectively. For both A and B, experiments were performed in triplicate and S.D. values were never greater than 5% of the mean.

3.8. Inhibition of rhodesain by vinyl sulfone and peptidyl epoxide inhibitors

Earlier peptidyl and peptidomimetic irreversible inhibitors used to target African trypanosome cysteine proteases have focused on interactions with the non-prime subsites (particularly S_2) in the active site cleft [13]. As part of an ongoing program to develop new cysteine protease inhibitors targeting rhodesain, cruzain and additional cysteine proteases of other important parasitic organisms, we tested a series of vinyl sulfonyl inhibitors [60] that were designed to explore the S′ subsites of rhodesain ΔC (Table 1). Cruzain was included in each assay for comparison. A number of inhibitors with a single-atom spacer between the sulfonyl group and a phenyl moiety were tested (R = OPh, CH_2Ph or NHPh) and compared with an inhibitor with the same phenyl substituent, but without a spacer (R = Ph). For both rhodesain ΔC and cruzain, the inhibitor with R = OPh is most potent with 20- and 30-fold greater activities, respectively, compared with the in-

hibitor without a spacer (R = Ph). With R = CH_2Ph, the activity drops to 2–3-fold compared with the inhibitor with R = Ph, and extending the length of the spacer to two carbons (R = CH_2CH_2Ph) led to a further 5–10-fold decrease in activity. The inhibitor with R = NHPh is rejected by rhodesain ΔC, being 6–7-fold less active than the inhibitor with R = Ph, whereas for cruzain there is a 2-fold loss of activity. The simple ethyl ester (R = OEt) compared with the phenoxy substituted inhibitor (R = OPh) is significantly less potent against both enzymes. Interestingly, switching the R-group from Ph to 2-pyridyl resulted in a 10- and 5-fold increase in inhibitor activity against rhodesain and cruzain, respectively. Qualitatively, therefore, the two enzymes react similarly to this series of vinyl sulfonyl inhibitors. Studies of additional inhibitor analogs in the R = OPh and R = 2-pyridyl series as potential drug candidates appear warranted based on these promising enzyme inhibition data.

Further comparative analysis of rhodesain and cruzain was performed using a series of peptidyl epoxide inhibitors based on the natural product E-64 as a lead structure [61]. The design, synthesis and evaluation of these E-64 analogs as inhibitors of cruzain are described elsewhere [62,63]. We have studied the effects of varying the P_2 amino acid side chain X and the terminal substituent R that extends into the S′ area (Table 2). The side chains of the amino acids L-leucine (Leu), L-homophenylalanine (homoPhe) and L-homotyrosine (homoTyr) are presumed to interact with the S_2 subsite, by analogy to the interaction of the leucine side chain in E64c with papain [64]. This series of inhibitors, in the main, was less potent than the vinyl sulfone series. Both proteases preferred the L-stereoisomer of homophenylalanine, leucine and homotyrosine when R was a simple OH group. Extending the terminal R substituent into the S′ sites, as exemplified by X = L-homoPhe, R = $NHOCH_2Ph$, abolished inhibition. However, inhibitor activity could be rescued by changing the P_2 amino acid from the L-isomer to the D-isomer. Finally, the inhibitor based on D-homoTyr with R = $NHOCH_2Ph$ discriminated cruzain from rhodesain the most (13-fold). Indeed, this inhibitor seems thus far selective for cruzain as lower second order rate constants were also measured for bovine cathepsin B, 2228 ± 323 (k_{ass}); papain, 1300 ± 539 (k_{ass}) and *L. major* cathepsin B, 83 600 ± 11 756 (k_{inact}/K_i) (E. Hansell, unpublished results).

Table 1
Inhibition of rhodesain ΔC and cruzain by peptidomimetic vinyl sulfone inhibitors and their derivatives designed to probe the S′ subsites

R-group[a]	k_{ass} (M^{-1} s^{-1})	
	Rhodesain	Cruzain
Ph	268 200 ± 44 760	596 400 ± 116 400[b]
OPh	5 808 000 ± 1 656 000	16 802 082 ± 340 000
NHPh	37 300 ± 7104	246 000 ± 84 400
CH_2Ph	891 000 ± 27 300	1 398 000 ± 294 000
CH_2CH_2Ph	181 800[c]	149 400 ± 15 000
OEt	129 000 ± 30 000	153 000 ± 24 000
2-Pyridyl	2 910 000 ± 396 000	3 417 600 ± 225 600

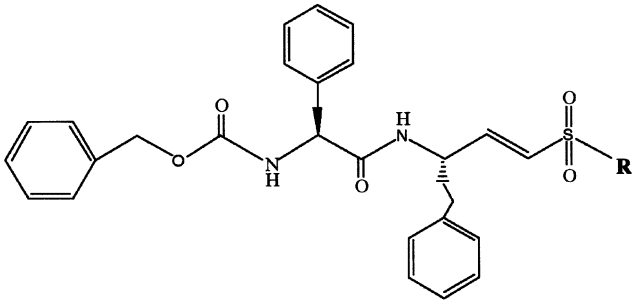

Recombinant rhodesain ΔC and cruzain (prepared according to [20]) were tested at concentrations of 2 nM. Tests were in duplicate or triplicate (with S.D. values). Concentration of substrate Z-Phe-Arg-AMC was 5 μM.
[a] R-group refers to the structure depicted above.
[b] k_{inact}/K_i value.
[c] k_{obs}/I value.

Table 2
Inhibition of rhodesain ΔC and cruzain by peptidyl epoxide inhibitors

X-group[a]	R-group[b]	k_{ass} (M^{-1} s^{-1})	
		Rhodesain	Cruzain
D-homoPhe	OH	3804 ± 624	4584 ± 984[c]
L-homoPhe	OH	75 720 ± 27 576[d]	57 750 ± 1836[d]
D-Leu	OH	8274 ± 1800	5016 ± 2304
L-Leu	OH	92 232 ± 4686[d]	65 700 ± 13 698[d]
D-homoTyr	OH	12 618 ± 5412	17 706 ± 1272
D-homoPhe	$NHOCH_2Ph$	93 702 ± 6504[d]	98 466 ± 9102[d]
L-homoPhe	$NHOCH_2Ph$	n.i.[e]	n.i.
D-homoTyr	$NHOCH_2Ph$	34 020 ± 6180	441 600 ± 57 760

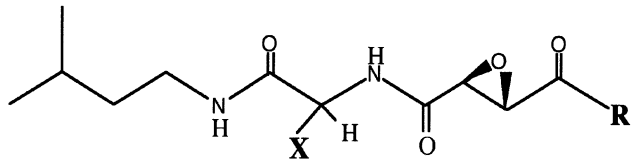

Recombinant rhodesain ΔC and cruzain (prepared according to [20]) were tested at 2 nM. Tests were performed in triplicate (S.D. values included). Concentration of substrate Z-Phe-Arg-AMC was 5 μM.
[a] Refer to the group X, of the structure depicted above.
[b] Refer to the group R, of the structure depicted above.
[c] k_{inact}/K_i value.
[d] k_{obs}/I, at lowest [I] significantly different from control.
[e] No inhibition, i.e. the values were no different from controls with dimethylsulfoxide (DMSO) alone up through 10 μM I.

3.9. Homology-based modeling of rhodesain

Based on homology modeling of rhodesain on cruzain, there are no sequence differences in the vicinity of the active site binding region that can explain the quantitative differences in the kinetic behavior between the enzymes with the vinyl sulfone and epoxide inhibitors. The only notable sequence changes within a 7 Å sphere of the active site region occur near the S_3 site, where Ser^{186} of cruzain is replaced by phenylalanine in rhodesain, and at the base of the S_2 cleft, where glutamate (Glu^{333}) is changed to alanine. Phenylalanine in S_3 can potentially make constructive hydrophobic interactions with the aromatic blocking group of the vinyl sulfone inhibitors. However, as the blocking group was held constant in all of the vinyl sulfone inhibitors tested, this does not explain the observed kinetic results. Glutamate found at the base of the S_2 cleft in cruzain is positioned away from the binding cleft and does not interfere with the hydrophobic interactions of the phenyl moiety of the inhibitor at P_2 as judged from numerous vinyl sulfone-bound cruzain structures [38], as well as other cruzain structures [59]. Therefore, the presence of alanine at the same position in rhodesain should not markedly affect inhibition potential. We can only conclude at this stage that allosteric effects are involved in the inhibition specificity of the two enzymes. The impact of sequence changes in loops as well as in buried regions at a distance from the active site cleft will be assessed from an X-ray crystal structure of the rhodesain $Asn^{295} \rightarrow Ala$ mutant, an effort currently in progress (L. Brinen, unpublished results).

Acknowledgements

We thank Jason P. Salter for advice and Christopher Franklin for technical assistance. This research was supported by a Charles E. Culpeper Biomedical Pilot Initiative Award to C.R.C. and by NIH Grant AI 35707 to J.H.M. and W.R.R. J.H.M. is supported by a Molecular Parasitology Scholar Award from the Burroughs Wellcome Foundation.

References

[1] Molyneux DH. Current public health status of trypanosomiasis and leishmaniasis. In: Hide G, Mottram JC, Coombs GH, Holmes PH, editors. Trypanosomiasis and Leishmaniasis: Biology and Control. Oxford: CAB International, 1997:39–50.
[2] WHO. Control and Surveillance of African Trypanosomiasis WHO Technical Report Series 881. Geneva: World Health Organisation, 1998.
[3] Kristjanson PM, Swallow BM, Rowlands GJ, Kruska RL, de Leeuw PN. Measuring the costs of African animal trypanosomosis, the potential benefits of control and returns to research. Agric Syst 1999;59:79–98.
[4] Croft SL, Urbina JA, Brun R. Chemotherapy of human leishmaniasis and trypanosomiasis. In: Hide G, Mottram JC, Coombs GH, Holmes PH, editors. Trypanosomiasis and Leishmaniasis: Biology and Control. Oxford: CAB International, 1997:245–57.
[5] Iten M, Matovu E, Brun R, Kaminsky R. Innate lack of susceptibility of Ugandan *Trypanosoma brucei rhodesiense* to DL-alpha-difluoromethylornithine (DFMO). Trop Med Parasitol 1995;46:190–4.
[6] Olson JE, Lee GK, Semenev A, Rosenthal PJ. Antimalarial effects in mice of orally administered peptidyl cysteine protease inhibitors. Bioorg Med Chem 1999;7:633–8.
[7] Engel JC, Doyle PS, Hsieh I, McKerrow JH. Cysteine protease inhibitors cure an experimental *Trypanosoma cruzi* infection. J Exp Med 1998;188:725–34.
[8] Selzer PM, Pingel S, Hsieh I, et al. Cysteine protease inhibitors as chemotherapy: lessons from a parasite target. Proc Natl Acad Sci USA 1999;96:11015–22.
[9] McKerrow JH, Engel JC, Caffrey CR. Cysteine protease inhibitors as chemotherapy for parasitic infections. Bioorg Med Chem 1999;7:639–44.
[10] Lonsdale-Eccles JD, Grab DJ. Lysosomal and non-lysosomal peptidyl hydrolases of the bloodstream forms of *Trypanosoma brucei brucei*. Eur J Biochem 1987;69:467–75.
[11] Authié E. Trypanosomiasis and trypanotolerance in cattle: a role for congopain. Parasitol Today 1994;10:360–4.
[12] Troeberg L, Pike RN, Morty RE, Berry RK, Coetzer THT, Lonsdale-Eccles JD. Proteases from *Trypanosoma brucei brucei*. Purification, characterisation and interactions with host regulatory molecules. Eur J Biochem 1996;238:728–36.
[13] Troeberg L, Morty RE, Pike RN, et al. Cysteine proteinase inhibitors kill cultured bloodstream forms of *Trypanosoma brucei brucei*. Exp Parasitol 1999;91:349–55.
[14] Scory S, Caffrey CR, Stierhof Y-D, Ruppel A, Steverding D. Trypanosoma brucei: killing of bloodstream forms in vitro and in vivo by the cysteine proteinase inhibitor Z-Phe-Ala-CHN_2. Exp Parasitol 1999;91:327–33.
[15] Caffrey CR, Scory S, Steverding D. Cysteine proteinases of trypanosome parasites: novel targets for chemotherapy. Curr Drug Targets 2000;1:155–62.
[16] Mottram JC, North MJ, Barry JD, Coombs GH. A cysteine proteinase cDNA from *Trypanosoma brucei* predicts an enzyme with an unusual C-terminal extension. FEBS Lett 1989;258:211–5.
[17] Åslund L, Henriksson J, Campetella O, Frasch AC, Pettersson U, Cazzulo JJ. The C-terminal extension of the major cysteine proteinase (cruzipain) from *Trypanosoma cruzi*. Mol Biochem Parasitol 1991;45:345–7.
[18] Sakanari JA, Nadler SA, Chan VJ, Engel JC, Leptak C, Bouvier J. Leishmania major: comparison of the cathepsin L- and B-like cysteine protease genes with those of other trypanosomatids. Exp Parasitol 1997;85:63–76.
[19] Smith S, Gottesman M. Activity and deletion analysis of recombinant human cathepsin L expressed in *Escherichia coli*. J Biol Chem 1989;264:20487–95.
[20] Eakin AE, Mills AA, Harth G, McKerrow JH, Craik CS. The sequence, organization, and expression of the major cysteine protease (cruzain) from *Trypanosoma cruzi*. J Biol Chem 1992;267:7411–20.
[21] Pamer EG, Davis CE, Eakin A, So M. Cloning and sequencing of the cysteine protease cDNA from *Trypanosoma brucei rhodesiense*. Nucleic Acids Res 1990;18:6141.
[22] Ausubel A, Brent R, Kingston RE, et al. Short Protocols in Molecular Biology, 4th ed. New York: Wiley, 1999.
[23] Laemmli UK. Cleavage of structural proteins during the assembly of the head of bacteriophage T4. Nature 1970;227:680–5.
[24] Van Meirvenne N, Janssens PG, Magnus E. Antigenic variation in syringe passed populations of *Trypanosoma* (*Trypanozoon*)

brucei I. Rationalization of the experimental approach. Ann Soc Belg Med Trop 1975;55:1–23.
[25] Lanham SM, Godfrey DG. Isolation of salivarian trypanosomes from man and other mammals using DEAE–cellulose. Exp Parasitol 1970;28:521–34.
[26] Brun R, Schoeneberger M. Cultivation and in vitro cloning of procyclic culture forms of *Trypanosoma brucei* in a semi-defined medium. Acta Trop 1979;36:289–92.
[27] Obexer W, Schmid C, Brun R. Activity and structure relationship of acridine derivatives against African trypanosomes. Trop Med Parasitol 1995;46:45–8.
[28] Hirumi H, Hirumi K. Continuous cultivation of *Trypanosoma brucei* blood stream forms in a medium containing a low concentration of serum protein without feeder cell layers. J Parasitol 1989;75:985–9.
[29] Bogyo M, Shin S, McMaster JS, Ploegh H. Substrate binding and sequence preference of the proteasome revealed by active-site-directed affinity probes. Chem Biol 1998;5:307–20.
[30] Bogyo M, Verhelst S, Bellingard-Dubouchaud V, Toba S, Greenbaum D. Selective targeting of lysosomal cysteine proteases with radiolabeled electrophilic substrate analogs. Chem Biol 2000;7:27–38.
[31] Tokuyasu KT. Use of poly(vinylpyrrolidone) and poly(vinyl alcohol) for cryoultramicrotomy. Histochem J 1989;21:163–71.
[32] Slot JW, Geuze HJ. A new method of preparing gold probes for multiple-labeling cytochemistry. Eur J Cell Biol 1985;38:87–93.
[33] Brickman MJ, Balber AE. *Trypanosoma brucei rhodesiense*: membrane glycoproteins localized primarily in endosomes and lysosomes of bloodstream forms. Exp Parasitol 1993;76:329–44.
[34] Griffiths G. Fine Structure Immunocytochemistry. Berlin: Springer, 1993.
[35] Eisenthal R, Cornish-Bowden A. The direct linear plot. A new graphical procedure for estimating enzyme kinetic parameters. Biochem J 1974;139:715–20.
[36] Barrett AJ, Kembhavi AA, Brown MA. L-*trans*-epoxysuccinyl-leucylamido(4-guanidino)butane (E-64) and its analogues as inhibitors of cysteine proteinases including cathepsins B, H and L. Biochem J 1982;201:189–98.
[37] Bieth JG. Theoretical and practical aspects of proteinase inhibition kinetics. Methods Enzymol 1995;248:59–84.
[38] Brinen LS, Hansell E, Cheng J, Roush WR, McKerrow JH, Fletterick RJ. A target within the target: probing cruzain's P1′ site to define structural determinants for the Chagas' disease protease. Structure 2000;8:831–40.
[39] Sali A, Blundell TL. Comparative protein modelling by satisfaction of spatial restraints. J Mol Biol 1993;234:779–815.
[40] Chappell CL, Dresden MH. *Schistosoma mansoni*: proteinase activity of "hemoglobinase" from the digestive tract of adult worms. Exp Parasitol 1986;61:160–7.
[41] Wang B, Shi GP, Yao PM, Li Z, Chapman HA, Brömme DJ. Human cathepsin F. Molecular cloning, functional expression, tissue localization, and enzymatic characterization. J Biol Chem 1998;273:32000–8.
[42] Brömme D, Li Z, Barnes M, Mehler E. Human cathepsin V. Functional expression, tissue distribution, electrostatic surface potential, enzymatic characterization, and chromosomal localization. Biochemistry 1999;38:2377–85.
[43] Pamer EG, Davis CE, So M. Expression and deletion analysis of the *Trypanosoma brucei rhodesiense* cysteine protease in *Escherichia coli*. Infect Immun 1991;59:1074–8.
[44] Fish WR, Nkhungulu ZM, Muriuki CW, Ndegwa DM, Lonsdale-Eccles JD, Steyaert J. Primary structure and partial characterization of a life-cycle-regulated cysteine protease from *Trypanosoma* (*Nannomonas*) *congolense*. Gene 1995;161:125–8.
[45] Martinez J, Henriksson J, Rydaker M, Cazzulo JJ, Pettersson U. Genes for cysteine proteinases from *Trypanosoma rangeli*. FEMS Microbiol Lett 1995;129:135–41.
[46] Wex T, Levy B, Wex H, Brömme D. Human cathepsins F and W: a new subgroup of cathepsins. Biochem Biophys Res Commun 1999;259:401–7.
[47] Karrer KM, Peiffer SL, DiTomas ME. Two distinct gene subfamilies within the family of cysteine protease genes. Proc Natl Acad Sci USA 1993;90:3063–7.
[48] Cygler M, Mort JS. Proregion structure of members of the papain superfamily. Mode of inhibition of enzymatic activity. Biochemie 1997;79:645–52.
[49] Mottram JC, Robertson CD, Coombs GH, Barry JD. A developmentally regulated cysteine proteinase gene of *Leishmania mexicana*. Mol Microbiol 1992;6:1925–32.
[50] Mottram JC, Frame MJ, Brooks DR, Tetley L, Hutchison JE, Souza AE, et al. The multiple cpb cysteine proteinase genes of *Leishmania mexicana* encode isoenzymes that differ in their stage regulation and substrate preferences. J Biol Chem 1997;272:14285–93.
[51] Omara-Opyene AL, Gedamu L. Molecular cloning, characterization and overexpression of two distinct cysteine protease cDNAs from *Leishmania donovani chagasi*. Mol Biochem Parasitol 1997;90:247–67.
[52] Pamer EG, So M, Davis CE. Identification of a developmentally regulated cysteine protease of *Trypanosoma brucei*. Mol Biochem Parasitol 1989;33:27–32.
[53] Mbawa ZR, Gumm ID, Fish WR, Lonsdale-Eccles JD. Endopeptidase variations among different life-cycle stages of African trypanosomes. Eur J Biochem 1991;195:183–90.
[54] Mbawa ZR, Gumm ID, Shaw E, Lonsdale-Eccles JD. Characterisation of a cysteine protease from bloodstream forms of *Trypanosoma congolense*. Eur J Biochem 1992;204:371–9.
[55] Mason RW, Green GD, Barrett AJ. Human liver cathepsin L. Biochem J 1985;226:233–41.
[56] Okenu DMN, Opara KN. *Trypanosoma brucei*: properties of extracellularly released proteases. J Parasit Dis 1996;20:17–22.
[57] Lonsdale-Eccles JD, Mpimbaza GWN, Nkhungulu ZR, et al. Trypanosomatid cysteine protease activity may be enhanced by a kininogen-like moiety from host serum. Biochem J 1995;305:549–56.
[58] Schechter I, Berger A. On the size of the active site in proteases. I. Papain. Biochem Biophys Res Commun 1967;27:157–62.
[59] Gillmor SA, Craik CS, Fletterick RJ. Structural determinants of specificity in the cysteine protease cruzain. Protein Sci 1997;6:1603–11.
[60] Roush WR, Gwaltney SL II, Cheng J, Scheidt KA, McKerrow JH, Hansell E. Vinyl sulfonate esters and vinyl sulfonamides: potent, irreversible inhibitors of cysteine proteases. J Am Chem Soc 1998;120:10994–5.
[61] Hanada K, Tamai M, Yamagishi M, Ohmura S, Sawada J, Tanaka I. Isolation and characterization of E-64, a new thiol protease inhibitor. Agric Biol Chem 1978;42:523–8.
[62] Roush WR, Alvarez Hernandez A, Zepeda G. A new synthesis of peptidyl epoxysuccinates for probing cysteine protease-inhibitor P-3/S-3 binding interactions, Synthesis 1999:1500–4.
[63] Roush WR, Alvarez Hernandez S, McKerrow JH, Selzer PM, Hansell E, Engel JC. Design, synthesis and evaluation of D-homophenylalanyl epoxysuccinate inhibitors of the trypanosomal cysteine protease cruzain. Tetrahedron 2000;56:9747.
[64] Yamamoto D, Matsumoto K, Ohishi H, et al. Refined x-ray structure of papain E-64-c complex at 2.1-Å resolution. J Biol Chem 1991;266:14771–7.